cigre Turkey

TEPES
TURKISH JOURNAL OF ELECTRICAL POWER AND ENERGY SYSTEMS

TEPES, Vol. 5, Issue. 2, 125-131, 2025 **DOI:** 10.5152/tepes.2025.24037

RESEARCH ARTICLE

Design of Electrodynamic Suspension System for Hyperloop Pod

Ibrahim Enes Uslu[1,2], Ahmet Selim Akkas[3], Mehmet Onur Gulbahce[4], Ilhan Kocaarslan[3]

[1]Department of Electronics and Communication Engineering, İstanbul Technical University, İstanbul, Türkiye
[2]Department of Artificial Intelligence and Data Fusion, Turkish Aerospace Industries, Ankara, Türkiye
[3]Department of Robotics and Autonomous Systems Engineering, İstanbul Technical University, İstanbul, Türkiye
[4]Department of Electrical Engineering, İstanbul Technical University, İstanbul, Türkiye

Cite this article as: I. Enes Uslu, A. Selim Akkas, M. Onur Gulbahce and I. Kocaarslan, "Design of electrodynamic suspension system for hyperloop pod," *Turk J Electr Power Energy Syst.*, 2025; 5(2), 125-131.

ABSTRACT

Hyperloop technology, introduced in 2013, is a revolutionary transportation concept designed to achieve near-supersonic speeds of approximately 1220 km/h for long-distance travel. The key factor enabling the Hyperloop capsule to reach such high speeds is that the system is exposed to minimal friction. This study focuses on the design of an electrodynamic suspension disc for the levitation system of a Hyperloop capsule to be used in the Hyperloop Development Competition hosted by The Scientific and Technological Research Council of Türkiye (TUBITAK) Rail Transportation Technologies Institute (RUTE). The levitation system utilizes a high-speed rotating permanent magnet to generate magnetic forces that lift and stabilize the capsule above the rail. Following the completion of the analytical design, the system was simulated using the finite element method in ANSYS Electronics Desktop, and necessary geometric and electrical optimizations were performed based on the simulation results. Finally, the system was implemented, and the experimental results were analyzed to validate the design.

Index Terms—Electrodynamic suspension, finite element analysis (FEA), hyperloop, levitation

I. INTRODUCTION

With the increasing pace of daily life in recent years, the need for faster and more efficient transportation systems has become paramount. To address this demand, air transportation, known for its high-speed capabilities, has often been the preferred choice. In land transportation, one of the primary limitations to speed is the friction force between wheels and the ground. Hyperloop technology, based on reducing friction forces, represents a state-of-the-art advancement by combining the principles of Maglev trains with vacuum tunnels. This system aims to achieve near-supersonic speeds of up to 1220 km/h on land [1–4]. In a study conducted by Hansen [3], hyperloop technology was compared with existing high-speed transportation vehicles such as aircraft, high-speed train, Transrapid, SCMaglev, and Swiss-metro. It was stated that although Hyperloop technology was limited in terms of carrying capacity and economic feasibility, it stood out with its energy efficiency and high-speed potential.

The Hyperloop capsule minimizes air resistance through its vacuum environment and eliminates ground friction using an advanced suspension system. This design allows most of the consumed energy to be converted directly into speed. A representative illustration of the Hyperloop concept is provided in Fig. 1.

The proposed Hyperloop system is envisioned as a next-generation transportation method, achieving unprecedented speeds under its current operating conditions [1, 2]. Moreover, its reliance on electrical energy rather than fossil fuels with significant carbon footprints underscores its environmentally friendly nature [2, 3, 5–9].

Suspension systems in transportation technologies can generally be categorized into three main groups: air cushioning vehicle (ACV) systems, electromagnetic suspension (EMS) systems, and electrodynamic suspension (EDS) systems.

In the first method, in air cushioning systems, suspension is achieved by blowing pressurized air from the vehicle to the ground through tubes or fans. While ACV systems provide a stable and low-friction ride at a relatively more affordable cost for short-distance travel [10–12], they are not considered suitable for long-distance transportation [12]. Additionally, introducing air into a vacuumed Hyperloop

Corresponding author: Mehmet Onur Gulbahce, **E-mail:** ogulbahce@itu.edu.tr

Received: December 26, 2024
Revision Requested: January 19, 2025
Last Revision Received: January 28, 2025
Accepted: December 31, 2024
Publication Date: March 10, 2025

Fig. 1. Hyperloop concept [5].

tunnel would compromise the vacuum, necessitating continuous re-vacuuming, which significantly reduces system efficiency.

The second method, EMS, achieves suspension using electromagnet systems installed on the guide rail or ferromagnetic systems paired with electromagnets on the train, powered by electric currents. Electromagnetic suspension requires an active control mechanism to maintain stability. For these reasons, EMS constantly consumes energy, and especially at high speeds, the amount of energy required by the electromagnets increases significantly [4, 13]. In these systems, suspension is provided through attractive magnetic forces [13, 16].

The third method, which is the focus of this study, is EDS. Electrodynamic suspension provides magnetic levitation by creating eddy currents and is usually designed with Halbach arrangements. Unlike EMS, EDS provides stability passively. Electrodynamic suspension offers energy efficiency and is suitable for ultra-high speeds [4, 13, 17]. Unlike EMS, EDS systems rely on repulsive magnetic forces to achieve suspension [14, 16]. In the system examined in this study, suspension is achieved through the repulsive forces generated by moving magnets interacting with the passive guide plates.

Main Points

- The paper focuses on designing and optimizing an electrodynamic suspension system for a Hyperloop capsule. This system uses rotating magnets to generate magnetic lift forces, enabling the contactless suspension of the capsule above the rail.
- The design process begins with analytical calculations and is further optimized using the finite element method (FEM). Key parameters such as magnetic forces, magnet geometry, and placement are analyzed in detail to enhance system performance.
- Simulation results are compared with experimental data to validate the design. While the results generally align, discrepancies are observed, particularly due to challenges in modeling the unstable air gap in the FEM simulations.

In this study, an EDS system was designed for a Hyperloop capsule with a weight of 70 kg. This study was conducted for the Hyperloop Development Competition organized by The Scientific and Technological Research Council of Türkiye (TUBITAK) Rail Transportation Technologies Institute (RUTE), which started in 2022 and is held every year. The project teams exhibit their Hyperloop prototypes in the competition. Firstly, the operating principle of the system was outlined, and the mathematical model was developed. Finite element analysis (FEA) was then conducted to optimize the system's analytical design and evaluate its performance against the specified requirements. Finally, a test setup was built to compare the practical results with the analytical and simulation-based findings.

II. DESIGN OF LEVITATION SYSTEM FOR HYPERLOOP POD

In EDS systems, suspension can be achieved through various methods, with the fundamental approach involving the generation of a variable magnetic field. This variable magnetic field can be created by moving the magnets, which not only facilitates suspension but also generates magnetic drag. At low speeds, magnetic drag is the dominant force, whereas suspension becomes predominant at higher speeds [18].

To achieve effective suspension in EDS systems, the magnets must move at high speeds, and this movement can be either linear or rotational. For the capsule designed in this study to remain suspended not only during motion but also while stationary, it is essential for the magnets to rotate. To enable this, a rotational platform was designed, as illustrated in Fig. 2, providing variability in the magnetic field through circular motion.

Eddy currents are generated when a conductive plate is subjected to a varying magnetic field [19]. Given that the peak magnetic flux applied to the conductor is denoted as φ_B, the magnetic flux induced in the disc can be expressed as a sinusoidal function. Using this representation, the steady-state expression for eddy currents is derived and presented in (2) [20].

$$\phi_B = \phi_0 \sin(wt) \tag{1}$$

$$i_{ss}(t) = \frac{\phi_0}{L} \cdot \frac{1}{1+\left(\frac{R}{wL}\right)^2} \cdot \left\{ \sin(wt) + \frac{R}{wL}\cos(wt) \right\} \tag{2}$$

The lift force and drag force generated in the system can be calculated using the following approaches [21, 22]. Here, B_0 denotes the maximum flux density at the surface, where $y = g$.

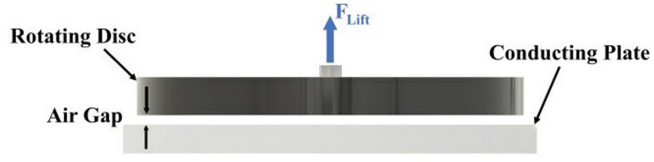

Fig. 2. Side view of the disc and plate.

$$B_z = B_0 \cdot \sin(kz) \cdot e^{-k(g-y)} \quad (3)$$

$$B_y = B_0 \cdot \cos(kz) \cdot e^{-k(g-y)} \quad (4)$$

The induced flux φ can be represented by the thickness of the conductor d and the width of the magnets in the direction of motion *w* (m) [21].

$$\phi = \frac{w \cdot B_0}{k} \cdot e^{-kg} \cdot \sin(kz) \cdot \left\{1 - e^{-kd}\right\} \quad (5)$$

Additionally, the current in the horizontal (x) direction is determined by substituting the maximum flux value into the steady-state Eddy current formula, as defined in (2), using (5).

$$I_x(z) = \frac{\lambda B_0 w}{2\pi L} \cdot \frac{1}{1+\left(\frac{R}{wL}\right)^2} \cdot e^{-kg} \cdot \left\{\sin(kz) + \frac{R}{wL}\cos(kz)\right\} \quad (6)$$

Then, the following force equations are formed by making use of the magnetic fields (3) and (4) created by the rotating magnets and the current generated in the horizontal plane (5).

$$\overline{F_y} = w\overline{I_x}(z) \times \overline{B_z} \quad (7)$$

$$\overline{F_z} = w\overline{I_x}(z) \times \overline{B_y} \quad (8)$$

As a result of averaging the magnitudes of the forces according to the wavelength, the average force magnitudes F_y and F_z are obtained [20].

Lift force:

$$F_y = \frac{B_0^2 w^2}{2kL} \cdot \frac{1}{1+\left(\frac{R}{wL}\right)^2} \cdot e^{-2kg} \quad (9)$$

Drag force:

$$F_z = \frac{B_0^2 w^2}{2kL} \cdot \frac{\left(\frac{R}{wL}\right)}{1+\left(\frac{R}{wL}\right)^2} \cdot e^{-2kg} \quad (10)$$

The primary objective in disc design is to maximize the lift force to enable the system to lift heavier loads. However, it is equally important to account for the drag force generated during operation. The efficiency of the system is typically expressed as the ratio of the lift force to the drag force [20]. This efficiency ratio can be calculated by simply dividing (9) by (10). During the design process, efforts were focused not only on increasing the lift force but also on improving the lift/drag ratio (11). This ratio was analyzed in detail, and various methods were applied to maximize its value.

$$\frac{F_y}{F_z} = \frac{wL}{R} = \frac{2\pi}{\lambda} \cdot v_z \cdot \frac{L}{R} \quad (11)$$

The competition setup prepared by the TUBITAK RUTE consists of a 208-meter-long tunnel, which is allowed to be used by the competitors. The design parameters determined according to the requirements and constraints given in the competition are presented in Table I.

III. THREE-DIMENSIONAL TRANSIENT MAGNETIC MODEL

Although magnetic suspension systems are modeled based on specific formulas and theories, solving these formulas and the associated differential equations can be challenging.

Due to the geometric complexity, certain equations cannot be solved symbolically. In such cases, numerical methods are employed. Finite element method is one of the most effective approaches, where systems are divided into a finite number of elements, and the equations are solved incrementally to approximate the solution. In this study, the FEM was applied to solve the equations defined between (12) and (18).

The magnetic flux density B and electric field intensity E are expressed as in (12) and (13), respectively, where V is the scalar electric potential, A is the magnetic vector potential, and *w* is the speed [23].

$$B = \nabla \times A \quad (12)$$

$$E = -\frac{\partial A}{\partial t} - \nabla.V + w \times \nabla \times A \quad (13)$$

Neglecting V, Ohm's law (14), Ampere's law, and the expression in (13) are used to achieve the expression in (15). Then, the divergence of (15) is taken to obtain (16) [23].

$$\vec{J} = \sigma\vec{E} \quad (14)$$

TABLE I.
GEOMETRIC AND ELECTRICAL PARAMETERS OF LEVITATION SYSTEM

Parameter	Symbol	Value
Pole number	P	3
Total magnet number	s	6
Mechanical air gap	g	8 mm
Angular velocity	w	4000 rpm
Disc diameter	d	145 mm
Distance of magnets from disk center	u	35 mm
Magnet diameter	m_d	30 mm
Magnet height	m_h	10 mm
Steel plate diameter	s_d	145 mm
Steel plate thickness	s_h	3 mm
Resulting moment	τ	1.5 Nm
Resulting lift force	F	100 N

$$\nabla \times -\frac{1}{\mu} \times \nabla \times A = \sigma\left(-\frac{\partial A}{\partial t} - w \times \nabla \times A + \nabla . V\right) \quad (15)$$

$$\nabla . \sigma\left(-\frac{\partial A}{\partial t} - w \times \nabla \times A + \nabla . V\right) = 0 \quad (16)$$

The scalar electric potential is expressed in terms of A and w as in (17). By substituting (13) into (15), it can be reached (18).

$$V = A.w \quad (17)$$

$$\nabla \times -\frac{1}{\mu} \times \nabla \times A = \sigma\left(-\frac{\partial A}{\partial t} - w.\nabla A - (A.\nabla)w - A \times (\nabla \times w)\right) \quad (18)$$

In this study, analytical calculations, such as those required for eddy currents induced by rotating magnets and the resulting lift force, are highly complex. Therefore, the FEM is essential. The magnetic model of the suspension system and the calculation of the forces generated were performed using ANSYS Electronics Desktop.

The three-dimensional (3D) transient magnetic model of the designed suspension disc is shown in Figs. 3 and 4. In the 3D transient magnetic model, the magnets were selected as NdFe-35. These magnets were arranged on the suspension disc with alternating polarities. The rail material was Aluminum 6101-T6 as in the competition setup prepared by the TUBITAK RUTE, while the steel components were made from Steel-1010.

Adding a steel plate to the system increases the magnetic flux density by channeling and concentrating the magnetic flux. Since steel is a ferromagnetic material, it provides a path for the magnetic flux to pass through. Normally, the magnetic flux would be distributed across the upper surface of the disk, but with the addition of the steel plate, the flux completes its circuit through the steel, thereby intensifying the magnetic field, as shown in Fig. 5. This increase in magnetic flux also results in a corresponding increase in the lift force.

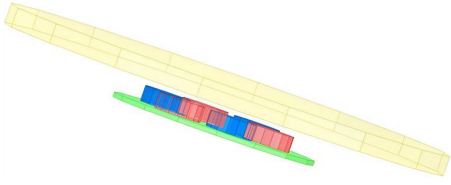

Fig. 3. Levitation disc geometry.

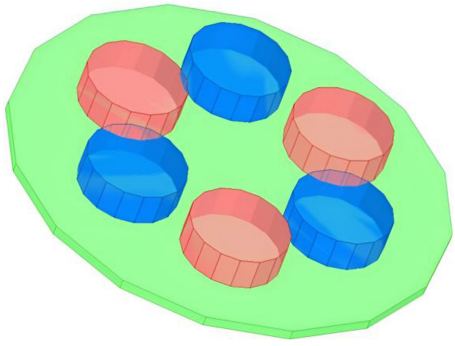

Fig. 4. Steel plate and magnet geometry.

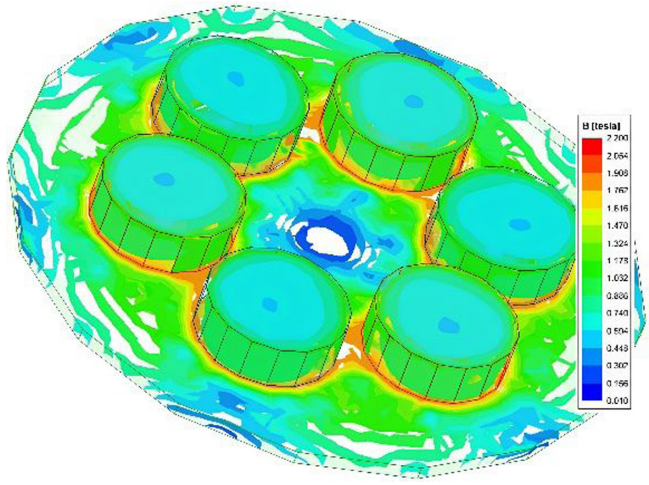

Fig. 5. Magnetic flux density distribution on magnets and plate.

Moreover, the upward magnetic fields generated by the system, which would normally propagate toward the capsule, can interfere with the electronic components inside. By placing a steel plate on the disk, these magnetic fields are redirected and contained within the steel, preventing them from directly reaching the capsule. This design minimizes the magnetic noise affecting the electronic

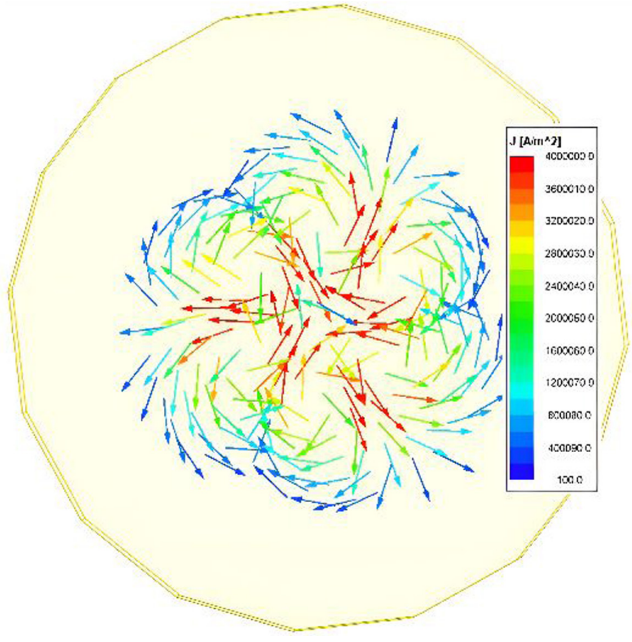

Fig. 6. Vector image of eddy currents occurring on the rail.

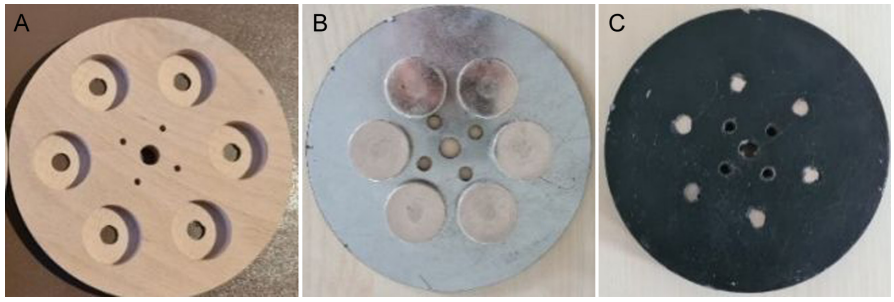

Fig. 7. (a) Sample suspension disk without magnet attached. (b) Placement of sheet metal and magnets. (c) Sample disk created with magnet, steel, and MDF.

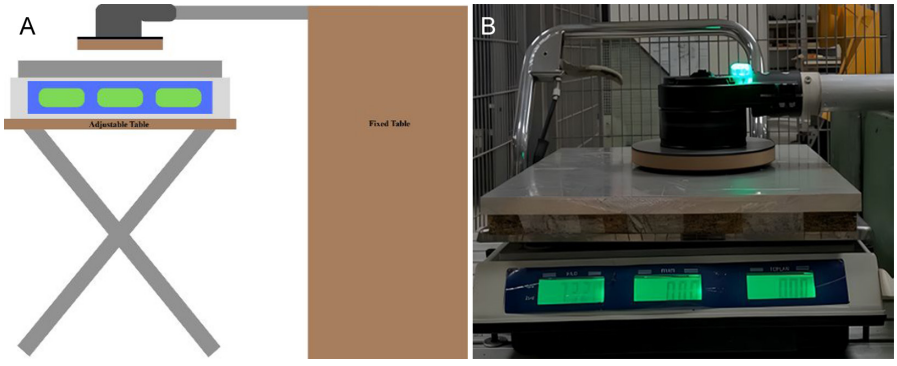

Fig. 8. Test setup: (a) Principle diagram. (b) Scale with mounted aluminum plate and disk structure.

components inside the capsule, enhancing system reliability. The current density observed on the rail is illustrated in Fig. 6.

IV. TEST RESULTS AND DISCUSSION

A basic experimental setup was established to evaluate the performance of the proposed system. The disk shown in Fig. 7 was manufactured according to the design parameters specified in Table I.

This levitation disk consists of six magnets arranged with alternating poles, ensuring that each magnet's pole is opposite to its neighboring magnets. The magnets have a diameter of 30 mm, a height of 10 mm, and are positioned 35 mm from the center of the disk, which has a total diameter of 145 mm. A steel plate with a matching diameter of 145 mm was added to the top of the disk to concentrate the magnetic flux, as illustrated in Fig. 7. The completed disk assembly was mounted onto a brushless DC motor and rotated at a speed of 4000 rpm for testing.

The mechanism shown in Fig. 8 is set up to measure the resulting lift force. A fixed, heavy table was placed on the right side of the mechanism to ensure stability during suspension. A pipe attached to this table holds the brushless motor at its end. On the left side of the mechanism, a hydraulic bench with adjustable height allows precise control of the air gap. An aluminum plate was mounted on a scale fixed to this bench. In addition, since the system consists of a mechanism that rotates at high speed, the system was tested in a metal cage, as seen in Fig. 8, until enough tests were done to ensure that the system was safe.

A laser tachometer was used to monitor the rotational speed of the brushless motor. The accuracy of the scale, which served as the measurement device in the test, was verified by measuring materials with predetermined masses. Therefore, there is no issue regarding the accuracy of the equipment used. However, due to the working principle of the scale, compression occurs as the force exerted by the disk on the aluminum plate increases. While the height of the disk

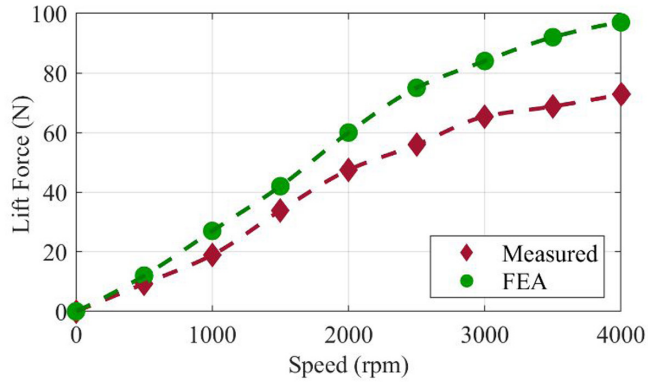

Fig. 9. Comparison of measured and FEA results of lift force as speed changes.

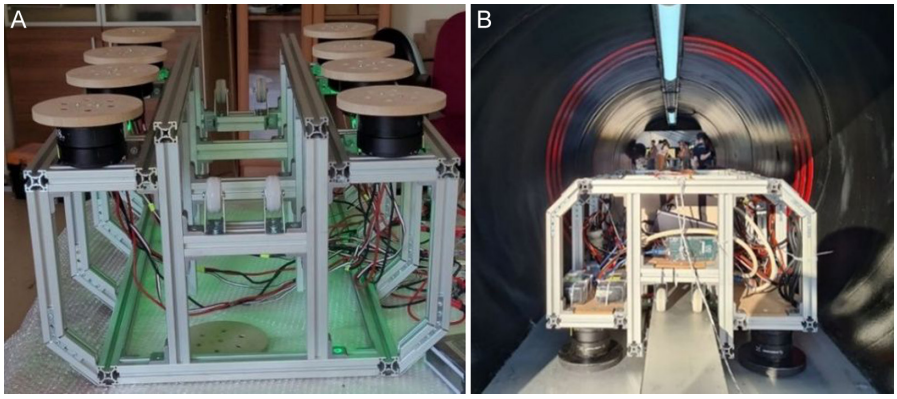

Fig. 10. Photo of the designed hyperloop capsule (a) reverse view and (b) positioned in tunnel.

remains fixed, this compression on the plate's surface causes the air gap to vary during the tests.

The results obtained from the test setup were analyzed, and a comparison between the experimental and simulation (FEA) results is presented in Fig. 9. Both the measured and simulated data indicate that the lift force increases with rotational speed (RPM). However, accurately modeling the unstable air gap observed in the test setup within the FEM framework remains challenging, leading to discrepancies between the experimental and simulation results.

Following the tests, eight suspension disks were installed at the base of the prototype. A reverse view of the capsule suspension system is illustrated in Fig. 10(a). Additionally, Fig. 10(b) shows a photograph of the completed capsule positioned in the test tunnel.

V. CONCLUSION

In this study, a basic EDS system was designed and produced for a 70 kg Hyperloop capsule prepared for the Hyperloop Development Competition organized by the RUTE of TUBITAK. The analytical design process was examined in detail, and its mathematical background was provided. After the analytical design was made, improvements were made to the model using the FEM. As a result of the design and subsequent optimizations, the rotating EDS system was completed. Then, an experimental device was produced, and experiment is made. The optimization of the designed system was performed within a limited scope due to competition constraints. It was observed that the magnetic losses resulting from the magnet arrays and shapes were significant. The effects of magnet shape, magnet arrangement, and magnet material on system performance, which are excluded from the scope of this study, need to be investigated in more detail.

Future studies could focus on a more comprehensive optimization of the system, including advanced finite element modeling and experimental validation to further minimize magnetic losses. Additionally, investigating the effects of alternative magnet geometries, arrangements, and materials on system efficiency and performance can provide valuable insights for enhancing the EDS system.

Availability of Data and Materials: The data that support the findings of this study are available on request from the corresponding author.

Peer-review: Externally peer-reviewed.

Author Contributions: Concept – I.E.U., A.S.A.; Design – I.E.U., A.S.A., M.O.G; Supervision – M.O.G., İ.K.; Resources – I.E.U., A.S.A., M.O.G; Materials – I.E.U., A.S.A.; Data Collection and/or Processing – I.E.U., A.S.A.; Analysis and/or Interpretation – M.O.G.; Literature Search –I.E.U; Writing – I.E.U, M.O.G.; Critical Review – M.O.G.

Declaration of Interests: Mehmet Onur Gulbahce is a member of the Advisory Board of Turkish Journal of Electrical Power, however, his involvement in the peer review process was solely as an author. Other authors have no conflicts of interest to declare.

Funding: This study was supported by İstanbul Technical University (İTU) Scientific Research Projects Unit (BAP) under Project MGA-2022-43948.

References

1. E. Musk, *Hyperloop Alpha*, 2013.
2. C. Timperio, *Linear Induction Motor (Lim) for Hyperloop Pod Prototypes* Master's thesis. ETH Zurich, Institute of Electromagnetic Fields (IEF), 2018.
3. I. A. Hansen, "Hyperloop transport technology assessment and system analysis," *Transp. Plan. Technol.*, vol. 43, no. 8, pp. 803–820, 2020. [CrossRef]
4. L. Mitropoulos, A. Kortsari, A. Koliatos, and G. Ayfantopoulou, "The hyperloop system and stakeholders: A review and future directions," *Sustainability*, vol. 13, no. 15, p. 8430, 2021. [CrossRef]
5. A. Silic, "'What Is Hyperloop and When Will It Be Ready?', discover magazine," 2022. [Online]. Available: https://www.discovermagazine.com/technology/what-is-hyperloop-and-when-will-it-be-ready. [.Accessed: 07 Oct, 2022].
6. R. Galluzzi *et al.*, "A multi-domain approach to the stabilization of electrodynamic levitation systems," *J. Vib. Acoust.*, vol. 142, no. 6, p. 061004, 2020. [CrossRef]
7. E. E. Dudnikov, "Advantages of a new hyperloop transport technology," in Tenth International Conference Management of Large-Scale System Development (MLSD). New York, United States of America: IEEE, 2017, pp. 1–4. [CrossRef]
8. J. K. Nøland, "A reality check on maglev technology for the hyperloop transportation system: Status update after a decade of development," *IEEE Access*, vol. 12, pp. 162918–162928, 2024. [CrossRef]

9. J. R. Dhobale, and S. Sahu, "Hyperloop transportation system," *Int. J. Innov. Eng. Res. Technol.*, pp. 1–3, 2018.
10. V. A. Kumar, G. Prajwal, F. Khan, C. Kapai, and N. Varun, "Design and development of hyperloop train," *Int. J. Res. Eng. Sci. Manag.*, vol. 3, pp. 235–238, 2020.
11. A. E. Hodaib, and S. F. A. Fattah, "Conceptional design of a hyperloop capsule with linear induction propulsion system," *Int. J. Aerosp. Mech. Eng.*, vol. 10, no. 5, pp. 997–1005, 2016.
12. F. H. Pelle, and S. R. Magdalena, *Air Cushion Vehicle (Acv): History Development and Maglev Comparison*, vol. 5, no. 1, 2019, pp. 5–25.
13. J. K. Nøland, "Prospects and challenges of the hyperloop transportation system: A systematic technology review," *IEEE Access*, vol. 9, pp. 28439–28458, 2021. [CrossRef]
14. M. N. O. Sadiku, and C. M. Akujuobi, "Magnetic levitation," *IEEE Potentials*, vol. 25, no. 2, pp. 41–42, 2006. [CrossRef]
15. R. Borcherts, and L. Davis, "Lift and drag forces for the attractive electromagnetic suspension systems," *IEEE Trans. Magn.*, vol. 10, no. 3, pp. 425–428, 1974. [CrossRef]
16. L. Zhu, and C. R. Knospe, "Modeling of nonlaminated electromagnetic suspension systems," *IEEE ASME Trans. Mechatron.*, vol. 15, no. 1, pp. 59–69, 2009.
17. S. Choi, C. Lee, and J. Lim, "Analysis of guidance and levitation forces between hts magnets and conductive tubes for hyperloop," *AIP Adv.*, vol. 14, no. 3, 2024. [CrossRef]
18. Y. Chen, W. Zhang, J. Z. Bird, S. Paul, and K. Zhang, "A 3-d analytic-based model of a null-flux halbach array electrodynamic suspension device," *IEEE Trans. Magn.*, vol. 51, no. 11, pp. 1–5, 2015. [CrossRef]
19. M. O. Gulbahce, D. A. Kocabas, and F. Nayman, "Investigation of the effect of pole shape on braking torque for a low power eddy current brake by finite elements method," in 8th International Conference on Electrical and Electronics Engineering (ELECO). New York, United States of America: IEEE, 2013, pp. 263–267. [CrossRef]
20. A. Lendek, and C. M. Apostoaia, "Investigation of an electrodynamic magnetic levitation device," in IEEE International Conference on Electro Information Technology (EIT). New York, United States of America: IEEE, 2020, pp. 297–303. [CrossRef]
21. R. F. Post, and D. Ryutov, *The Inductrack Concept: A New Approach to Magnetic Levitation*," tech. rep. Livermore, CA (United States): Lawrence Livermore National Laboratory (Lawrence Livermore National Laboratory, Office of Science), 1996.
22. R. F. Post, and D. D. Ryutov, "The inductrack: A simpler approach to magnetic levitation," *IEEE Trans. Appl. Supercond.*, vol. 10, no. 1, pp. 901–904, 2000. [CrossRef]
23. M. O. Gulbahce, D. A. Kocabas, and A. K. Atalay, "Determination of the effect of conductive disk thickness on braking torque for a low power eddy current brake," in New York, United States of America: IEEE, 2013, pp. 1272–1276. [CrossRef]